Accepted Manuscript

Recent results on Ion Cyclotron Wall Conditioning in mid and large size Tokamaks

D. Douai, A. Lyssoivan, V. Philipps, V. Rohde, T. Wauters, T. Blackman, V. Bobkov, S. Brémond, S. Brezinsek, F. Clairet, E. de la Cal, T. Coyne, E. Gauthier, T. Gerbaud, M. Graham, S. Jachmich, E. Joffrin, R. Koch, A. Kreter, R. Laengner, P.U. Lamalle, E. Lerche, G. Lombard, M. Maslov, M.-L. Mayoral, A. Miller, I. Monakhov, J.-M. Noterdaeme, J. Ongena, M.K. Paul, B. Pégourié, R.A. Pitts, V. Plyusnin, F.C. Schüller, G. Sergienko, M. Shimada, A. Sirinelli, W. Suttrop, C. Sozzi, M. Tsalas, E. Tsitrone, B. Unterberg, D. Van Eester

PII: S0022-3115(10)00791-9
DOI: 10.1016/j.jnucmat.2010.11.083
Reference: NUMA 45231

To appear in: *Journal of Nuclear Materials*

Received Date: 19 November 2010
Accepted Date: 29 November 2010

Please cite this article as: D. Douai, A. Lyssoivan, V. Philipps, V. Rohde, T. Wauters, T. Blackman, V. Bobkov, S. Brémond, S. Brezinsek, F. Clairet, E. de la Cal, T. Coyne, E. Gauthier, T. Gerbaud, M. Graham, S. Jachmich, E. Joffrin, R. Koch, A. Kreter, R. Laengner, P.U. Lamalle, E. Lerche, G. Lombard, M. Maslov, M.-L. Mayoral, A. Miller, I. Monakhov, J.-M. Noterdaeme, J. Ongena, M.K. Paul, B. Pégourié, R.A. Pitts, V. Plyusnin, F.C. Schüller, G. Sergienko, M. Shimada, A. Sirinelli, W. Suttrop, C. Sozzi, M. Tsalas, E. Tsitrone, B. Unterberg, D. Van Eester, Recent results on Ion Cyclotron Wall Conditioning in mid and large size Tokamaks, *Journal of Nuclear Materials* (2010), doi: 10.1016/j.jnucmat.2010.11.083

Recent results on Ion Cyclotron Wall Conditioning in mid and large size Tokamaks

D. Douai (*)[1], A. Lyssoivan[2], V. Philipps[3], V. Rohde[4], T. Wauters[1,2] T.Blackman[5], V. Bobkov[4], S. Brémond[1], S. Brezinsek[3], F. Clairet[1], E. de la Cal[6], T.Coyne[5], E. Gauthier[1], T.Gerbaud[5], M.Graham[5], S.Jachmich[2], E.Joffrin[1], R. Koch[2], A. Kreter[3], R. Laengner[3], P.U. Lamalle[7], E.Lerche[2], G. Lombard[1], M. Maslov[8], M.-L. Mayoral[5], A.Miller[5], I. Monakhov[5], J.-M. Noterdaeme[4,9], J. Ongena[2], M.K. Paul[3], B. Pégourié[1], R.A. Pitts[7], V. Plyusnin[10], F.C. Schüller[7], G. Sergienko[3], M. Shimada[7], A. Sirinelli[5], W. Suttrop[4], C.Sozzi[11], M.Tsalas[12], E. Tsitrone[1], B. Unterberg[3], D.Van Eester[2], the TORE SUPRA Team, the TEXTOR Team, the ASDEX Upgrade Team and JET EFDA Contributors*

[1]CEA, IRFM, Association Euratom-CEA, 13108 St Paul lez Durance, France.
[2]LPP-ERM/KMS, Association Euratom-Belgian State, 1000 Brussels, Belgium, TEC partner.
[3]IEF-Plasmaphysik FZ Jülich, Euratom Association, 52425 Jülich, Germany, TEC partner
[4]Max-Planck Institut für Plasmaphysik, Euratom Association, 85748 Garching, Germany.
[5]CCFE, Culham Science Centre, OX14 3DB, Abingdon, UK.
[6]Laboratorio Nacional de Fusión, Association Euratom-CIEMAT, 28040 Madrid, Spain.
[7]ITER International Organization, F-13067 St Paul lez Durance, France.
[8]CRPP-EPFL, Association Euratom-Confédération Suisse, CH-1015 Lausanne, Switzerland.
[9]Gent University, EESA Department, B-9000 Gent, Belgium.
[10]Centro de FNIST, Association Euratom-IST, 1049-001 Lisboa, Portugal.
[11]IFP-CNR, EURATOM-ENEA-CNR Fusion Association, Milano Italy.
[12]NCSR 'Demokritos', Athens, Greece
**See the Appendix of F. Romanelli et al., Proc. 22nd Int. FEC Geneva, IAEA (2008)*

Wall conditioning techniques applicable in the presence of permanent toroidal magnetic field will be required for the operation of ITER, in particular for recovery from disruptions, vent and air leak, isotopic ratio control, recycling control and mitigation of the tritium inventory build-up. Ion Cyclotron Wall Conditioning (ICWC) is one of the most promising options and has been the subject of considerable recent study on current tokamaks. This paper reports on the findings of such studies performed on European tokamaks, covering a range of plasma-facing materials: TORE SUPRA, TEXTOR, ASDEX Upgrade and JET.

JNM Keywords (5): P0500 Plasma-Materials Interaction , P0600 Plasma Properties

PSI-19 Keywords (5): ITER, Wall conditioning, Wall materials, Tritium removal.

Corresponding Author Address: David Douai, DSM/Institut de recherche sur la fusion par confinement magnétique, CEA Centre de Cadarache, 13108 Saint Paul lez Durance Cedex France

Corresponding Author e-mail: david.douai@cea.fr

Presenting Author: David Douai

Presenting Author e-mail: david.douai@cea.fr

Introduction

In ITER and future fusion devices, the magnetic field, generated by superconducting coils, will be continuously maintained. In the presence of such a magnetic field, conventional DC-glow discharges are unstable and can therefore no longer be used between ohmic plasma pulses. During the non-active He or H phase of ITER, with divertor targets made of carbon-fibre composite (CFC), interpulse wall conditioning will be required for reliable discharge initiation or recovery after disruptions. In the D:T phase, wall conditioning may also contribute to the control of the tritium inventory in ITER, of which the build-up is a major issue [1]. The Ion Cyclotron Wall Conditioning (ICWC) technique based on Radio-Frequency (RF) discharges is fully compatible with the presence of the magnetic field. The encouraging results obtained in current tokamaks using conventional Ion Cyclotron Resonance Frequency (ICRF) heating antennas [2-4], were recently acknowledged by the integration of ICWC into the ITER baseline using the ITER ICRF heating system [5]. Results obtained on EAST with dedicated RF antennas are also reinforcing ICWC [6]. However, new investigations are needed prior to its validation and its application to ITER, in particular for fuel removal, recovery after disruptions and isotopic ratio control.

This paper reviews the results of recent ICWC experiments performed on current tokamaks, covering a range of plasma-facing materials: TORE SUPRA (CFC), TEXTOR (fine-grain graphite), ASDEX-Upgrade (all W-coated wall) and JET (CFC/Be). The relevance of ICWC, specifications for its application to ITER and the operational domain on current tokamaks are introduced in the first part. The optimization of ICWC discharges is the subject of the second part. The third part reports on the assessment of the efficiency of D_2 (or H_2) and He-ICWC discharges for isotopic exchange and fuel removal. The benefit of pulsed ICWC discharges is treated in this part. The last part is devoted to the discussions of the experimental observations. In particular the He retention in metallic plasma-facing components (PFC) and the role of the different species in wall conditioning are discussed. The operation of ICWC and its efficiency for fuel removal are finally extrapolated to ITER.

1. ICWC experiments on the four tokamaks and ICWC discharge characterization

a. Principle and relevance of ICWC for wall conditioning

The principle of ICWC discharge production, in the presence of the toroidal magnetic field, has been described elsewhere (see e.g. [7]). The coupling of the RF power to the ICWC discharge is non-resonant and mainly results from the absorption of the RF energy by the electrons. Plasmas with densities ranging from 10^{16} and 10^{18} m^{-3} (i.e. 4 to 6 orders of magnitude higher than in DC glow discharges) and temperatures $1 < T_e < 10$ eV can be produced in a “relay-race” regime of slow and fast wave excitation [7] .

In the presence of an Ion Cyclotron Resonance (ICR) inside the torus, protons or deuterons can be accelerated by ICR heating at the major radius R where the resonance frequency of ions equals the wave frequency $\omega = qB_T(R)/M$, q being the charge of the ion, M its mass and B_T the toroidal magnetic field. In that case, and like in no other low temperature wall conditioning plasmas, fast neutrals, with temperatures above 1 keV and energies up to 50 keV, are created by charge exchange (CX) between the accelerated ions and the background neutral gas.

The admitted scheme for the interaction of ICWC discharges with the tokamak first wall results from previous theoretical analysis of D_2-ICWC discharges [8], in which it was shown that the main ion energy loss mechanism is CX reactions with neutrals. Hence, fluxes of fast CX neutrals to the walls comparable with those of ions accelerated in the cathode fall in DC-

Glow Discharge Conditioning (GDC) [3], but with a much higher energy, are bombarding the walls. They may have similar interaction depths than fluxes in tokamak plasmas, penetrating deeply in the subsurface of Plasma Facing Components (PFCs), where they could potentially access to deeply retained tritium atoms. They may also more easily break strong metal-oxide bonds like BeO on beryllium of JET with the ITER-Like Wall or ITER. Slow neutrals are created by dissociation of molecular hydrogen by electron collisions, these having Franck-Condon energies of a few eV, which, due to the low collisionality in the low density plasma, can only be lost at the walls. In this scheme, the main flux to the walls is therefore an isotropic neutral flux [8], which may be of advantage when remote or shadowed areas, like in the pump duct areas of the divertor or gaps, have to be conditioned.

b. Specifications of ICWC in ITER

In ITER, the use of ICWC during the interpulse period of nominal D:T plasma shots, in order to recover tritium as much as possible and prepare the wall for the next tokamak pulse, implies that the toroidal field is fixed at 5.3 T. With RF frequencies of the ICRH generators ranging from 40 to 55 MHz, ICR layers for D^+ ions lie in ITER on axis at $\rho = 0$, i.e. above the divertor, and at $\rho = -0.6$, respectively, with $\rho = r/a$ the normalized radius ($-1 \leq \rho \leq 1$). For such large distances d between the RF antenna and the ICR layer (d > 2.8m), the antenna coupling (defined as the fraction of the generator power coupled to the plasma, $\eta = P_{RF,coupled}/P_{RF,Generator}$) may be weak at $\eta < 40\%$ [7] .

The simulation of such a situation with ITER-relevant f/B_T values of 7.0 – 10.5 MHz/T [9] is only possible in JET, the largest existing tokamak (R = 2.96 m, a = 1.25 m) with divertor and an ITER-like geometry, at $B_T = 3.3$ T and f = 25 MHz, with on-axis $\omega = \omega_{CD}{}^+$.

This has been done with the present CFC walls, and in view of future comparative experiments after the installation of the ITER-Like Wall (ILW) [10].

The situation is identical in the non active He or H phase of ITER, with B_T=2.65 T, where ICR layers for the protons will also lie between ρ = 0 and ρ = -0.6. ITER half field ICWC scenarios have been simulated in the all tungsten tokamak ASDEX Upgrade (AUG), as well as in TORE SUPRA and TEXTOR at f/B_T ~15 MHz/T for on axis $\omega = \omega_{CH^+}$.

c. Main operational parameters of ICWC on the four tokamaks

The standard ICRF heating antennas of each device have been used. On JET, two of the four standard antennas (each having four straps) were used to couple between 50 to 250 kW RF power to the ICWC discharge, operated in He, D_2 or their mixtures. Gas injection was constant and JET cryopumps were used during ICWC. In order to improve the ICWC discharge uniformity and to extend the coverage to the divertor region, a small vertical magnetic field (up to 30 mT) has been successfully applied. On AUG, four ICRF antennas, consisting each of two poloidal current straps, were used with a total coupled power to the discharge, $P_{RF,coupled}$, between 100 and 250 kW. 6s long ICWC discharges have been operated in He:H_2 mixtures at pressures p = (1–8) · 10^{-2} Pa. Gas injection was constant for all experiments. ICWC discharge durations between 1s and 60s have been performed on TORE SUPRA in He, H_2 and their mixtures, taking advantage of its unique capability to sustain long discharge. Gas injection was either constant or feedback controlled on the pressure. RF powers between 25 and 250 kW were coupled to the plasma through a standard two straps antenna, either in continuous mode or in pulsed mode. Note that under given conditions (p > 10^{-1} Pa, $P_{RF,\ coupled}$ > 100 kW), arcing traces were observed on the TORE SUPRA antenna straps. However, these could be successfully operated for plasma heating after ICWC. The

TEXTOR ICWC discharges were operated at maximal hydrogen partial pressure with the help of feedback controlled injection (5.10^{-3} – 5.10^{-2} Pa) overlaid with a constant He flow. One or two ICRF antenna(s) were used with coupled RF powers between 15 and 60 kW in continuous mode. A small oscillating magnetic field has been successfully superimposed to the toroidal field at B_T = 1.92 T, allowing its vertical elongation in time.

Table 1 gives a summary of the ICWC discharge parameters used in the four tokamaks.

Table 1. ICWC discharge parameters foreseen in ITER and used in the four tokamaks

	Geometry	PFC	T (K)	R (m)	a (m)	B_T (T)	f (MHz)	P_{RF} (kW)	gas	p (Pa)
ITER (D:T)	Divertor	Be/W	373	6.2	2	5.3	40-55		He, D	
ITER (He H)		Be/C/W				2.65			He, H	
JET	Divertor	C (Be)	373	2.96	1.25	3.3	25	50-250	He, D	10^{-3} - 10^{-2}
AUG	Divertor	W	373	1.65	0.5	2 2.4	30 36.5	10-250	He, H	(1–8) · 10^{-2}
TORE SUPRA	Limiter	C	393	2.4	0.72	3.8 (3.2)	48	25-250	He, H	10^{-2} - 10^{-1}
TEXTOR	Limiter	C	373	1.75	0.47	1.92 (0.23-2.3)	29	15-60	He, H	5.10^{-3} – 5.10^{-2}

Since large amounts of fuel (e.g. deuterated or tritiated Beryllium co-deposits in the D:T phase) are expected in the divertor area of ITER, the crucial question of whether the ICWC discharge can reach the divertor region was addressed in JET as well as in AUG.

2. Homogenization and optimization of D_2-ICWC for fuel removal by isotope exchange

a. Characterization and homogeneity of ICWC discharges

ICWC discharges are low density and low temperature plasmas for which most of standard diagnostic tools of fusion plasmas are not well adapted. Plasma densities have however been measured either by means of interferometry or when available, by reflectometry (JET, TORE SUPRA). Local electron density and temperature were determined on TEXTOR from thermal Li beam emission [11]. Radial profiles of the electron radiation temperature were obtained from ECE radiometry on JET and AUG. ICWC discharges are known to be toroidally homogeneous [2]. However, in the absence of poloidal field, ICWC discharges are usually radially asymmetric and concentrated at the low field side (LFS) [8], with a large density gradient at LFS. Radial asymmetries are explained by ExB drifts [8], [12] and by the fact that fast magneto-sonic wave (FW) is non-propagating in low density ICWC plasmas [13]. Electron density profiles, measured by reflectometry on TORE SUPRA exhibit a radial decay from LFS towards the axis, more pronounced at low RF power, plasma density being proportional to the coupled RF power [2], [14]. Similarly, steep radial profiles of the radiative temperature T_{rad} of electrons were measured by means of ECE radiometry at the LFS of JET and AUG.

In all devices, the efficiency of ICWC was assessed by monitoring the partial pressures of the masses of interest, either using absolutely calibrated quadrupole mass spectrometers (QMS) or optical penning gauges (JET). In JET, the gas released from the regeneration of cryopumps after ICWC experiments was also analyzed by means of gas chromatography, allowing to perform a more accurate particle balance. The flux of high energy CX neutrals, produced by charge exchange with protons or deuterons accelerated in the ICR layer, were measured with a neutral particle analyzer (JET, TORE SUPRA, AUG). The charge exchange spectra of D and H atoms, measured on JET in a D_2 ICWC discharge are shown on Figure 1. The temperature of the fast CX neutral D and H atoms are 18 and 9 keV respectively, with a tail up to 60 keV for the protons.

b. Homogenization and effect on ICWC efficiency

The ICWC discharge uniformity can be improved by superimposing an additional vertical magnetic field on the toroidal field ($B_V << B_T$) [13]. Figure 2 shows two images from a wide angle visible CCD camera in two D_2-ICWC discharges on JET with identical parameters ($P_{RF,coupled}$ = 250kW, p = 2.10^{-3} Pa) in the absence (left picture) or the presence (right) of a small poloidal field (B_{POL} = 30 mT, B_{POL}/B_T ~1%). The addition of B_{POL} to the toroidal field, and in particular its vertical component, allowed by tilting the field lines, to elongate the ICWC discharge in vertical direction to top and bottom and to extend the coverage of the plasma to the divertor area, as seen on Figure 2. The radial component of B_{POL} improved radial uniformity of the discharge towards the high field side (HFS). The vertical and radial extension of the ICWC discharge in the presence of B_{POL} was confirmed by the line integrated density profiles measured on bottom horizontal and vertical cords at the HFS of the JET interferometer.

Besides homogenization, the addition of B_{POL} may enhance bombardment at the intersection points of the magnetic field lines with the wall [9], by ions which normally remain confined in the pure toroidal case. The extension of the coverage by the ICWC discharge is seen on the total pressure (shown on Figure 3), measured higher during the discharge and the post-discharge in the presence of B_{POL}, indicating that the ICWC discharge interacts with larger area.

Local electron densities and temperatures could be determined from Li beam emission spectroscopy in TEXTOR He:H_2 ICWC discharges in the presence of a small oscillating magnetic field $B_V \cos(\omega t) + B_R \sin(\omega t)$ ($|B_V| = |B_R|$ = 10 Gauss, ω = 10 Hz), superimposed to the toroidal field B_T = 1.92 T. The thermal Li beam is mounted into the limiter lock of TEXTOR, at the bottom of the device. Highest electron density and temperature and the resulting electron pressure p_e were measured when the oscillating field was purely vertical (B_R = 0), evidencing the vertical extension of the ICWC discharges towards the bottom of

TEXTOR in the presence of the solely vertical field component [11].

c. Optimization of ICWC discharge parameters

Efficiency of D_2 (resp. H_2) -ICWC discharge for isotopic exchange has already been reported in [3] and more recently in [15], where a significant modification (from 4 to 50%) of the isotopic ratio H/(H+D) was obtained after nearly 900s He-H_2 ICWC cumulated time on a wall preloaded by D_2-GDC. However, particle balance evidenced that H retention was on average ten times higher than D exhaust [15].

Strong H pumping of AUG tungsten PFCs during a He-H_2 ICWC discharge ($p = 5.10^{-2}$ Pa, $P_{RF,coupled} = 130$ kW) was also observed. This can be seen from the mass spectrometric signals of He, H_2 (red dots and black crosses, respectively) on Figure 4. The signal for HD molecules is given by the open blue squares. The black dashed and red dotted lines on Figure 4 are the calculated He and H_2 partial pressure levels in the absence of RF power. The signals of He, H_2, normalized to their respective pressure levels in the absence of RF power, show that almost all the hydrogen and an important fraction of the Helium injected are lost at the walls as the RF power is switched on. This last point will be discussed below.

In JET, the pressure and RF coupled power were adjusted to optimize the efficiency of D_2-ICWC discharges for fuel removal by isotopic exchange. Figure 5 shows the amount of out pumped H atoms (open blue squares) and the outpumping to retention ratio (red dots, right axis) as a function of the coupled RF power applied to the ICWC discharge for $p < 5.10^{-3}$ Pa and of the D_2-ICWC pressure for $150 < P_{RF,coupled} < 250$ kW. The best conditions to maximize the ratio between outpumping and retention (red dots on Figure 5) without lowering the H release were found to be high power (~250 kW) and low pressure (~2.10^{-3} Pa). The release of H atoms was found to increase with the H_2 partial pressure in the discharge, in agreement with similar increase of D outpumping in H_2-ICWC on TORE SUPRA in a somewhat higher pressure range (up to 8.10^{-2} Pa) [15]. In the case where p < 5.10^{-3} Pa, the behavior of the out pumped flux was found to weakly depend on the coupled RF power, as found in [3].

In He-ICWC discharges, D (or H) outpumping is strongly related to the coupled RF power in He-ICWC discharges, as shown on Figure 6a, where the H removal rate in TORE SUPRA He-ICWC discharges is plotted as a function of the coupled RF power. Removal rates are calculated over 2s active phase and 8s post-discharge. Two sets of data for walls either saturated with H_2-GDC and partly depleted during previous He ICWC (blue dots), or loaded by preceding H_2-ICWC discharges (red squares) illustrate the influence of the wall history on the conditioning efficiency. The increase of the removal rate with the RF power to the plasma is in agreement with [2], where the same behavior is reported for pulsed discharges, and consistent with the increase of both the electron and the He^+ densities with the RF power (Figure 6b, for the same pulses). This also indicates that in He-ICWC discharges, wall desorption is driven by He ion bombardment.

3. Assessment of the efficiency of ICWC plasmas

a. D_2-(H_2) ICWC discharges for fuel removal by isotopic exchange

In order to assess the efficiency for fuel removal by isotopic exchange on JET, the following procedure was adopted: two hours H_2-GDC was operated to preload the walls with ~4.10^{23} H atoms, after which the JET cryopumps were regenerated. Then, 8 identical D_2-ICWC discharges (p =2.10^{-3} Pa, B_V = 30mT, 9s duration) have been repeated in JET, the cryopumps were again regenerated and the gas released from the regeneration of cryopumps was analyzed by gas chromatography. Due to difficulties to couple the RF power to the plasma in the first discharges, the coupled power was varying between 50 and 250 kW.

The isotopic ratio measured either from optical penning gauges in the divertor or from midplane spectroscopy, is given on Figure 7 as a function of the cumulated discharge time. Both show an increase of the isotopic ratio D/(D+H) between 30 and 50% in a cumulated discharge time of 72s. The gas balance from gas chromatography (including both discharge and post discharge phases) yield $1.6.10^{22}$ H out gassed and $4.8.10^{22}$ D retained. The overall H outpumping is to be compared with the short term retention accessible by plasma operation: 2.10^{23} D atoms [16]. However, H_2 molecules released from the walls were weakly pumped by JET cryopumps. The H_2 saturated vapor pressure is in the 10^{-3} Pa range at 4.8 K, i.e. most of the time above the H_2 partial pressure in isotopic exchange experiments. Thus, the amount of H out pumped may be underestimated in the gas balance after regeneration of JET cryopumps.

b. He-ICWC discharges for fuel removal

Fuel removal rates ranging from 10^{16} to 3.10^{17} $D.m^{-2}.s^{-1}$ have been achieved in Helium ICWC discharges. The highest removal rate was measured on JET, after a set of He-D_2 ICWC discharges, in a 8s long pure He-ICWC discharge at a coupled RF power of 80 kW and a total pressure of 5.10^{-3} Pa. The rate was calculated including 30s post-discharge time. The Deuterium and Helium partial pressures in this ICWC discharge are shown on Figure 8 as a function of the discharge time. Note that in all He containing ICWC discharge on JET, a large fraction of He was found to be retained in the walls, as observed in AUG. This point will be discussed below.

c. Pulsed discharges

The probability f that a wall desorbed particle is ionized or dissociated and subsequently lost the walls before being pumped out and removed is high in ICWC discharges, where plasma density ranges between 10^{16} and 10^{18} m^{-3}. This probability can be written expressing the fact that the residence time of a desorbed specie $\tau \sim \tau_i = [n_e(k_{ion} + k_{diss})]^{-1}$, where k_{ion} and k_{diss} are the ionization and dissociation rates, respectively, is much shorter than its characteristic pumping time τ_S [2]: $f = \tau_i^{-1}/(\tau_S^{-1} + \tau_i^{-1}) \sim 1$. Hence, the out pumped flux is linked to the wall desorbed flux: $Q_{outpumped} = (1 - f)\, Q_{desorbed}$. For typical D_2 (or H_2) ICWC plasma density and temperature of 10^{17} m^{-3} and 3 to 5 eV, respectively, and using for k_{ion} and k_{diss} the values given in [17], one has $(1- f) < 10^{-3}$. Such a high reionization probability can explain low out pumping efficiency and high particle retention during the RF pulse [17]. Wall bombardment and subsequent desorption, followed by reionization of desorbed species, and finally particle retention, are only present when the RF power is on.

Short ICWC discharge pulses, followed by a pumping time, have to be used to reduce retention over a discharge and post-discharge cycle. In the post-discharge, only wall desorption occurs with a characteristic time scale (of the order of 1–10 s) depending on the physical process [18]. In order to optimize the fuel removal efficiency, the influence of the pulse duration on the outpumping was studied on TORE SUPRA in both D_2-ICWC and He-ICWC discharges. The results are shown on Figure 9 for the removal of D by H_2-ICWC discharge on walls saturated by a D_2-GDC. It clearly shows that it is possible to reduce the ratio between retention and outpumping (red dots, left axis) towards unity for sufficiently short pulse durations. The total amount of exhausted D with the discharge time, calculated over a complete cycle (discharge and post-discharge), with a post-discharge duration fixed to

30s, and given by the blue dots on Figure 9 (right axis), is also decreasing as the RF ON time decreases, but two times slower than the retention to outpumping ratio.

Pulsed He-ICWC discharges ($p = 4.10^{-2}$ Pa, $P_{RF,coupled} = 60$ kW) have been successfully applied on TORE SUPRA to recover normal operation after disruptions, when subsequent plasma initiation would not have been possible without conditioning [15]. The HD partial pressure in the Torus was found comparable with those obtained in low current ohmic pulsed discharges [19], which are routinely used on TORE SUPRA to recover from disruptions. The removal rates of HD molecules were typically $Q_{HD} \sim 1\text{-}2.10^{16}$ mol.m^{-2}.s^{-1} at low RF power [15].

4. Discussion

a. Importance of the vacuum pumping system

In He-ICWC, for the same coupled RF power per particle density $P/N = 8.10^{3}$ kW.Pa^{-1}.m^{-3}, and similar pulse durations (5s and 8s, respectively), a 10 times higher H out pumped flux was measured on JET than on TORE SUPRA (see Figure 6a and Figure 8). Assuming the same density and temperatures at the same P/N in both He-ICWC discharges, the out pumped flux depends only on the characteristics pumping time of a given specie (cf. 3.c): $Q_{outpumped} = \tau_S^{-1} / (\tau_S^{-1} + \tau_i^{-1})\, Q_{desorbed}$, and thus on the pumping speed. The difference is therefore easily explained by the different pumping speeds of D in JET and H in TORE SUPRA: $S(D_2) \sim 115$ m^3.s^{-1} in JET and $S(H_2) \sim 10$ m^3.s^{-1} in TORE SUPRA. Hence, proper choice of the vacuum pumping system is essential for the optimisation of the efficiency of ICWC.

b. He retention

In JET and AUG, a large fraction of the injected He was found to be retained in the walls during He containing ICWC discharges. Figure 8 shows the partial pressure of He and D, measured by optical penning gauges in a He-ICWC discharge on JET ($p=5.10^{-3}$ Pa, $P_{RF,\ coupled}$ = 80 kW). The red dashed line indicates the He puffing. From the partial pressures and the gas injection rates in this shot, it was found that 8.10^{20} He atoms were retained into JET walls. In the mean time, 10^{21} D atoms were released.

From the calculated particle balances of 11 successive He- containing ICWC discharges in JET, an average helium retained fraction of 80% was found, with a total retention of about 2.10^{21} He atoms. In the two first D_2-ohmic plasmas burned after this set, the He/D ratio was found to be as high as 4%. Two hours D_2-GDC and two additional ohmic plasmas brought the He/D ratio below 0.3%.

He retention has also been observed in all W AUG, as shown on Figure 5, and in a lesser extent in Tore Supra. In the first case, this observation is in agreement with the observed He storage in W materials by He glow discharges in laboratory experiments, and the high He plasma impurity concentrations reported in AUG following He-GDC [20].

The fraction of He retained is shown on Figure 6b in TORE SUPRA He-ICWC discharges at 2.10^{-2} Pa as a function of the coupled power. Each pulse of 2s was followed by 8s post-discharge. Also the line integrated electron density is shown on Figure 6b (green squares, right axis). Both the fraction of He retained and the electron density increase with the RF power to the plasma, indicating that retention occurs under He^+ ion bombardment. Clearly, the He retention is much lower than in JET, even at the higher coupled power per particle P/N = 200 $kW.Pa^{-1}.m^{-3}$ than in JET (40 $kW.Pa^{-1}.m^{-3}$).

Therefore, the explanation must be sought on the side of different materials in interaction with the ICWC discharge. In particular, the protection limiters of JET ICRF antennas, made of bulk beryllium, are possible candidate to explain such a high retention. Due to the radial inhomogeneity of the ICWC discharges, these are also in strong interaction with the He plasmas. Fractions of He retained to the total fluence close to unity in beryllium irradiated by Helium ions in the keV range are reported in e.g. [21].

In any case, it is important to assess to which extent He retention in W and Be PFCs of fusion devices can impact plasma operation after wall conditioning, either with ICWC or GDC.

c. Role of CX neutrals

The exact role of high energy CX neutrals in the isotopic exchange is still an open question [8]. On TEXTOR, the fast CX neutrals were suppressed in He-H_2 ICWC operated at low toroidal magnetic field (B_T = 0.23 T) at f = 29 MHz, where no ion cyclotron absorption for the protons at high cyclotron harmonics $\omega = n\omega_{cH}+$, n>>1 was predicted by 1-D RF modeling [13]. Figure 10 shows two CCD images of TEXTOR He-H_2 ICWC plasmas at nominal (2.3 T, left) and low (0.23 T, right) toroidal fields. Although the antenna coupling η was about 50% higher at low B_T, the same amount of out pumped and retained particles was obtained from particle balance at low B_T, compared to similar RF discharges at nominal field (B_T = 2.3 T).

From the CX D spectrum measured on JET with a neutral particle analyzer shown on Figure 1, (D_2-ICWC, p = 2.10^{-3} Pa, $P_{RF,coupled}$ = 280 kW), one can deduce Γ_{CX} = 3.10^{16} m^{-2}.s^{-1}. This apparently does not seem enough to explain retention nor desorption quantitatively. An illustration of this is given on Figure 11, where the out pumped H (black squares), the retained D (blue dots) and the integrated flux of fast (T_i ~10 keV with energies > 1keV) CX

D neutrals (open red dots), defined as $\int 4\pi S_{JET}\Gamma_{CX}dt$, (S_{JET} being the area of JET) are plotted as a function of the coupled RF power during the 8 identical D_2-ICWC discharges described in section 3.a. Coupling of the RF power was improved from shot to shot (see section 3.a), and was varying between 50 to 250 kW. The mean CX D neutral temperature is also shown (green squares, right axis) on Figure 11. Clearly, the measured fast CX D neutrals are one order of magnitude below outpumping and two orders of magnitude below retention. Moreover, whereas the fast CX flux and temperature T_D fairly exhibit a linear dependency on the RF power, the H release and the D retention remain unaffected by the variation of the RF power, as found in section 2.b in agreement with [3]. In these JET D_2-ICWC plasmas, the ionization degree is high ($\gamma = n_e/(n_e+N_0) \leq 1$), so that the RF power is essentially spent on increasing T_e. Since the probability $f = \tau_i^{-1}/(\tau_S^{-1}+\tau_i^{-1})$ that a wall desorbed particle is reionized and lost to the walls before being pumped out, increases with T_e, this may explain the fact that neither outpumping nor retention apparently depend on the fast CX flux. Moreover, due to the high cross section for charge exchange collisions (5.10^{20} m^2 between 5 and 10 keV), the mean free path along the field lines of high energy deuterons, created in the ICR layer in front of the ICRH antennas, is at most one meter at the considered pressure (2.10^{-3} Pa), i.e. smaller than the dimensions of the torus. This leads to toroidal and poloidal asymmetric distributions of fast CX neutrals. The line of sight of the NPA being 90° with respect to the ICRH antennas, the total fast CX D neutrals impinging onto the walls may be underestimated.

d. Extrapolation to ITER

Estimations of the ICWC power range in ITER has been done in [13] and [22], either from the extrapolation from present devices or with a 0-D code simulating the RF plasma production in the presence of toroidal and vertical magnetic fields. ICWC conditioning plasmas for inter-shot cleaning, recycling control and tritium removal by isotope exchange may be produced in ITER (a = 2.6 m, R=6.2 m, B_T=5.3 T, p = 2−8.10^{-2} Pa) for coupled RF powers ranging from 0.3 to 2 MW, depending on the gas pressure and on the RF power absorption scheme [22].

An extrapolation of hydrogen removal rates in ITER from those obtained in the present review is difficult, since only few minutes of cumulated ICWC durations either in continuous or pulsed mode have been operated. About 5 monolayers H atoms were removed within 72s cumulated D_2-ICWC on JET, which extrapolated to ITER would correspond to 0.25gT [23]. However, one should reasonably expect that the fuel removal efficiency will decrease with the ICWC operation time, as in GDC and as shown in [24]. Therefore, all the quantities given above allow only extrapolating upper limits of fuel removal rates to ITER. It should be again stressed that the high retention observed in ICWC discharge should be avoided by operating ICWC in a pulsed mode, and that further work should be done to assess the conditioning efficiency under this mode of operation.

Conclusion

Ion Cyclotron Wall Conditioning is a promising option for interpulse wall conditioning in future superconducting devices, such ITER. Considerable efforts have been brought to better characterize ICWC discharges, although most of the diagnostics used on TORE SUPRA, TEXTOR, ASDEX-Upgrade and JET, are not adapted to these low density and low temperature plasmas. Diagnostics dedicated to the monitoring and the control of ICWC plasma parameters during ITER operation will be necessary.

ICWC discharges suffer intrinsically from radial and poloidal inhomogeneities which can be corrected with the help of small radial and/or vertical magnetic fields. In the latter case, a vertical extension was experimentally confirmed on TEXTOR by means of Li beam emission spectroscopy. A similar homogenization was successfully obtained on JET, with an apparent increase of the ICWC plasma coverage towards both the divertor area and the central column, accompanied by an increase of the wall outgassing.

In D_2 (or H_2)-ICWC, the main fluxes to the walls are slow (with Franck-Condon energies of a few eV) and fast neutrals (energies in the keV range), which may be of advantage when remote or shadowed areas of tokamaks have to be conditioned. D_2-ICWC discharges efficiency have been optimized on JET walls saturated with H, with the double aim to maximize outpumping and to keep retention at the lowest level achievable. Low pressure and high RF power were found to fulfill these conditions. Hence an accurate assessment of D_2-ICWC for fuel removal by isotope exchange could be undertaken. An amount of H atoms equivalent to 10% of the short term retention could be removed from JET walls, at the price of a 3 times more D retention.

Fuel removal with He-ICWC, driven by He ion bombardment, was found to be less efficient than in D_2 (or H_2) ICWC. The highest fuel removal rates in He-ICWC discharges, at a given coupled power per particle were also reported on JET, evidencing the necessity to operate ICWC with the highest pumping speed available. Significant He retention is reported in both JET and AUG, a known issue in the latter case. The presence of Be as constituting materials of JET RF antenna protection limiters is suspected to be responsible for the 80% retained fraction of the He injected in ICWC discharges. It is stressed that in fusion devices with W and/or Be PFCs, the impact of He as conditioning gas on subsequent plasma operation should be assessed.

The flux of fast charge exchange neutrals (T in the keV range) measured by NPA in D_2

ICWC discharges on JET, was found too low to explain outpumping and retention quantitatively. The high reionization of wall desorbed particles in ICWC plasmas having densities between 10^{16} to 10^{18} m^{-3}, may explain the fact that neither outpumping nor retention apparently depends on the fast CX flux. However, the toroidal and poloidal asymmetries of the distribution of fast CX neutrals should be taken into account to assess their contribution. The role of the slow neutrals, having Franck-Condon energies of a few eV, should also be investigated.

It is shown, that pulsed ICWC discharges, studied on TORE SUPRA, allow to minimize the high retention to outpumping ratio in D_2 (or H_2) ICWC in continuous mode, where it is always higher than unity. For short pulses (<1s), retention may be lower than outpumping, without severely decreasing the isotope exchange efficiency. Such a very promising operation mode may be used in the superconducting tokamak ITER, and allow exchanging tritium by deuterium efficiently without saturating walls. However, the contribution of low energy neutrals in desorption and retention should be investigated in detail as well as possible synergistic effects with fast neutrals.

Further work on ICWC is hence needed to better characterize these discharges in terms of plasma parameters, fluxes to the walls and interaction with different PFC materials. In the view of such studies, JET with its ILW should offer a unique opportunity.

Acknowledgements

This work was supported by EURATOM and carried out within the framework of the European Fusion Development Agreement. The views and opinions expressed herein do not necessarily reflect those of the European Commission.

References

[1] J. Roth et al. Plasma Phys. Control. Fusion 50 (2008) 103001

[2] E. Gauthier, E. de la Cal, Journal of Nuclear Materials, Volumes 241-243, 11 February 1997, Pages 553-558

[3] E. de la Cal, E. Gauthier, Plasma Phys. Control. Fusion 39 (1997) 1083–1099

[4] J.S. Hu et al., Fusion Engineering and Design 82 (2007) 133–139

[5] A0 GDRD 3 01-07-19 R1.0, Design Requirements and Guidelines Level 2 (DRG2), ITER (2006)

[6] J.S. Hu, et al., J. Nucl. Mater. 376 (2008) 207-210

[7] A. Lyssoivan et al., Nuclear Fusion 32 (8) (1992) 1361

[8] E. de la Cal, Plasma Phys. Control. Fusion 48 (2006) 1455–1468

[9] C. Schueller, Report on Applications of ICWC on ITER, Contract number: IO/2009/ADM-014

[10] S. Brezinsek, this conference

[11] R. Laengner, this conference

[12] E. de la Cal, E. Gauthier, Plasma Phys. Control. Fusion 47 (2005) 197–218

[13] A. Lyssoivan et al., Volumes 390-391, 2009, Pages 907-910

[14] A. Lyssoivan et al., Problems of Atomic Science and Technology. 2007, 1. Series: Plasma Physics (13), p. 30-34

[15] D. Douai et al., 36th EPS Conference on Plasma Phys. Sofia, June 29 - July 3, 2009 ECA Vol.33E, P-4.200 (2009)

[16] T. Loarer, this conference

[17] T. Wauters, this conference

[18] V. Philipps, and J. Ehrenberg, J. Vac. Sci. Technol. 11 (1993) 437-445

[19] Grisolia C. et al., Vacuum 60 (2001) 147-152

[20] K. Schmid et al., Nucl. Fusion 47 (2007) 984–989

[21] K. Morishita et al., JNM 266-269 (1999)

[22] A. Lyssoivan, this conference

[23] M. Shimada, R.A. Pitts, this conference

[24] H.G. Esser J. Nucl. Mater. 241-243 (1997) 861

Figure captions

Figure 1

CX spectra of deuterium (red dots) and hydrogen (open blue squares) in a JET D_2-ICWC discharge, p=2.10^{-3} Pa, $P_{RF,\ coupled}$~ 280kW (JPN#79277)

Figure 2

Vertical and radial extension of JET ICWC discharge in the presence of a small poloidal field B_{POL}. Conditions are similar (D_2 ICWC, $P_{RF,coupled}$ = 250kW, p = 2.10^{-3} Pa) except B_{POL} =0 (left, JPN#79271), B_{POL} = 30 mT (right, JPN#79271).

Figure 3

Total pressure in the JET vacuum vessel in the absence (blue squares, JPN#79271) and in the presence (red dots, JPN#79271) of a small poloidal field B_{POL} = 30 mT.

Figure 4

Mass spectrometric signals (black dashed, red dotted), calculated injected pressures (black dashed, red dotted) and coupled RF power (green line) in a AUG He-H_2 ICWC discharge (p = 5.10^{-2} Pa, $P_{RF,coupled}$ = 130 kW)

Figure 5

H exhausted (open blue squares, left axis), and outpumping to retention ratio (red dots, right axis) as a function of the coupled RF power (right, p < 5.10^{-3} Pa), of the D_2 pressure (left, $P_{RF,coupled}$ > 150 kW) for a series of JET discharges.

Figure 6 - a (left) Dependency of H removal rates in 2s long TORE SUPRA He-ICWC discharges (p = 2.10^{-2} Pa) on coupled RF power, for walls saturated with H_2-GDC (blue dots), or loaded by preceeding H_2-ICWC (red dots) - b (right) Fraction of He retained (black dots, left axis) and line integrated electron density (green squares, right axis) in 2s long TORE SUPRA He-ICWC discharges at 2.10^{-2} Pa as a function of the coupled power.

Figure 7

Isotopic ratio as measured by optical penning gauges (red dots) in the divertor and from midplane spectroscopy (open blue squares) as a function of the cumulated D_2 ICWC discharge time in JET

Figure 8

Partial pressure of He and D, measured by optical penning gauges in a JET He-ICWC discharge on JET (p=5.10^{-3} Pa, $P_{RF,\ coupled}$ = 80 kW, JPN#78588).

Figure 9

D outpumping (blue, right axis) and ratio of retained H over D outpumping as a function of the pulse duration in a TORE SUPRA H_2-ICWC ($P_{RF,coupled}$~100 kW, p ~10^{-2} Pa, walls saturated by D-GDC)

Figure 10

Images of TEXTOR He-H_2 ICWC plasmas at nominal (2.3 T, left) and (0.23 T, right) toroidal fields, showing the position of the layers for the fundamental (B_T = 2.3 T) and the high harmonics of the ICR frequency (B_T = 2.3 T).

Figure 11

Out pumped H (black squares), retained D (blue dots), integrated flux of fast CX D neutrals (open red dots) and mean CX D neutral temperature (green squares, right axis) as a function of coupled RF power in 8 JET D_2-ICWC discharges. Conditions are described in section 2.b.

Figures

Figure 1

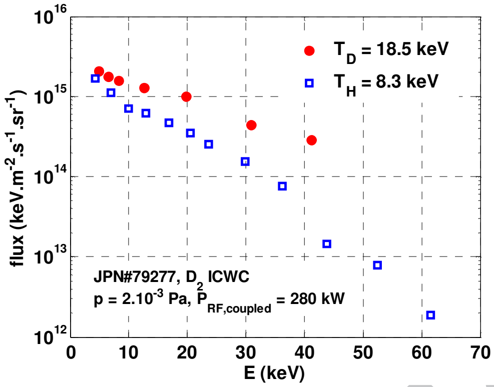

Figure 2

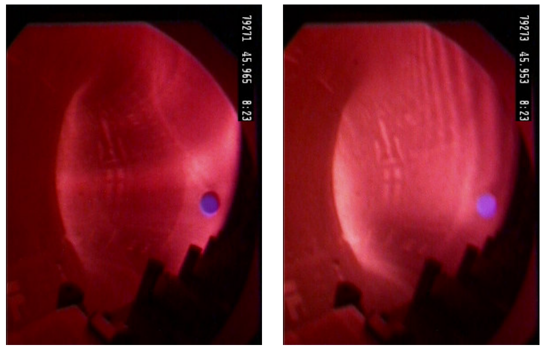

Figure 3

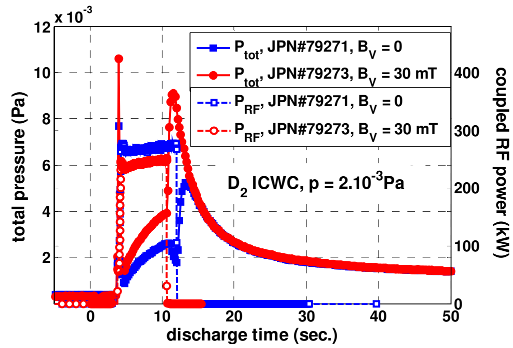
x 10^-3
total pressure (Pa)
coupled RF power (kW)
discharge time (sec.)
P_tot, JPN#79271, B_V = 0
P_tot, JPN#79273, B_V = 30 mT
P_RF, JPN#79271, B_V = 0
P_RF, JPN#79273, B_V = 30 mT
D_2 ICWC, p = 2.10^-3Pa

Figure 4

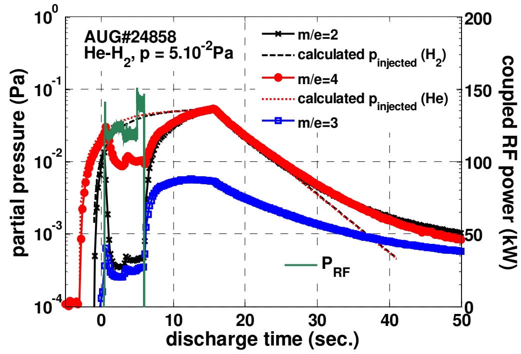
AUG#24858
He-H2, p = 5.10-2Pa
m/e=2
calculated p injected (H2)
m/e=4
calculated p injected (He)
m/e=3
PRF
partial pressure (Pa)
coupled RF power (kW)
discharge time (sec.)
10^0
10^-1
10^-2
10^-3
10^-4
200
150
100
50
0
0
10
20
30
40
50

Figure 5

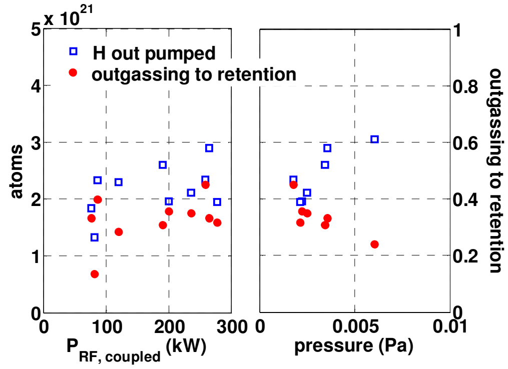
x 10^21
H out pumped
outgassing to retention
atoms
outgassing to retention
P_RF, coupled (kW)
pressure (Pa)
0
1
2
3
4
5
100
200
300
0.005
0.01
0.2
0.4
0.6
0.8

Figure 6

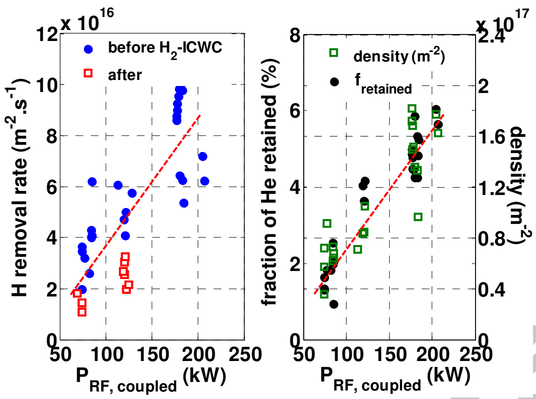
x 10^16
before H2-ICWC
after
H removal rate (m^-2.s^-1)
P_RF, coupled (kW)
x 10^17
density (m^-2)
f_retained
fraction of He retained (%)
density (m^-2)
P_RF, coupled (kW)

Figure 7

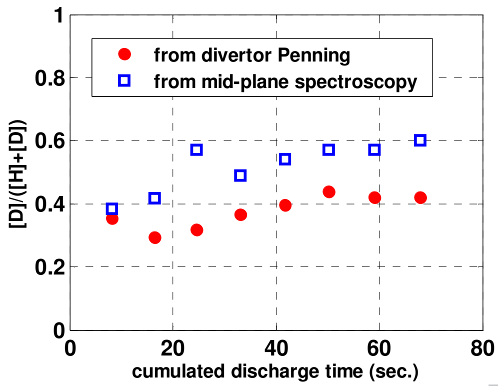
from divertor Penning
from mid-plane spectroscopy
[D]/([H]+[D])
cumulated discharge time (sec.)
0
0.2
0.4
0.6
0.8
1
0
20
40
60
80

Figure 8

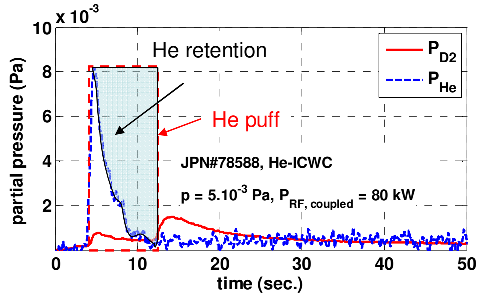
x 10-3
He retention
He puff
PD2
PHe
JPN#78588, He-ICWC
p = 5.10-3 Pa, PRF, coupled = 80 kW
partial pressure (Pa)
time (sec.)
0
10
20
30
40
50
2
4
6
8
10

Figure 9

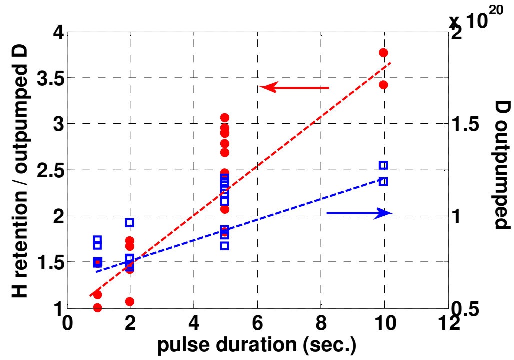
x 10^20
4
3.5
3
2.5
2
1.5
1
2
1.5
1
0.5
0
2
4
6
8
10
12
H retention / outpumped D
D outpumped
pulse duration (sec.)

Figure 10

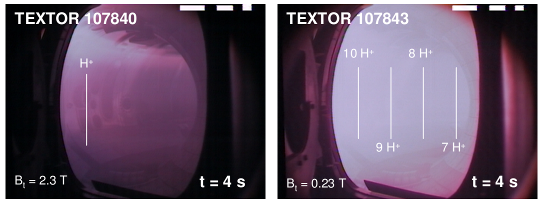
TEXTOR 107840
H+
Bt = 2.3 T
t = 4 s
TEXTOR 107843
10 H+
8 H+
9 H+
7 H+
Bt = 0.23 T
t = 4 s

Figure 11

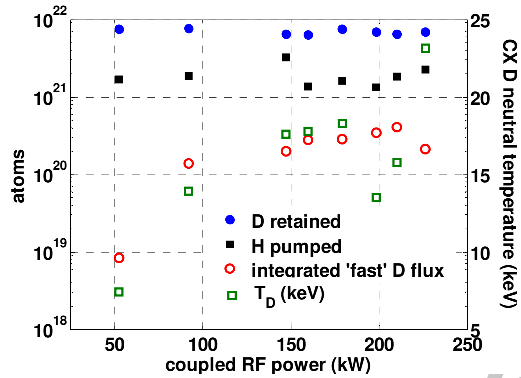

atoms
CX D neutral temperature (keV)
coupled RF power (kW)
D retained
H pumped
integrated 'fast' D flux
T_D (keV)
10^{22}
10^{21}
10^{20}
10^{19}
10^{18}
25
20
15
10
5
50
100
150
200
250

Table 1. ICWC discharge parameters foreseen in ITER and used in the four tokamaks

	Geometry	PFC	T (K)	R (m)	a (m)	B_T (T)	f (MHz)	P_{RF} (kW)	gas	p (Pa)
ITER (D:T)	Divertor	Be/W	373	6.2	2	5.3	40-55		He, D	
ITER (He H)		Be/C/W				2.65			He, H	
JET	Divertor	C (Be)	373	2.96	1.25	3.3	25	50-250	He, D	10^{-3} - 10^{-2}
AUG	Divertor	W	373	1.65	0.5	2 2.4	30 36.5	10-250	He, H	$(1–8) \cdot 10^{-2}$
TORE SUPRA	Limiter	C	393	2.4	0.72	3.8 (3.2)	48	25-250	He, H	10^{-2} - 10^{-1}
TEXTOR	Limiter	C	373	1.75	0.47	1.92 (0.23-2.3)	29	15-60	He, H	5.10^{-3} – 5.10^{-2}